

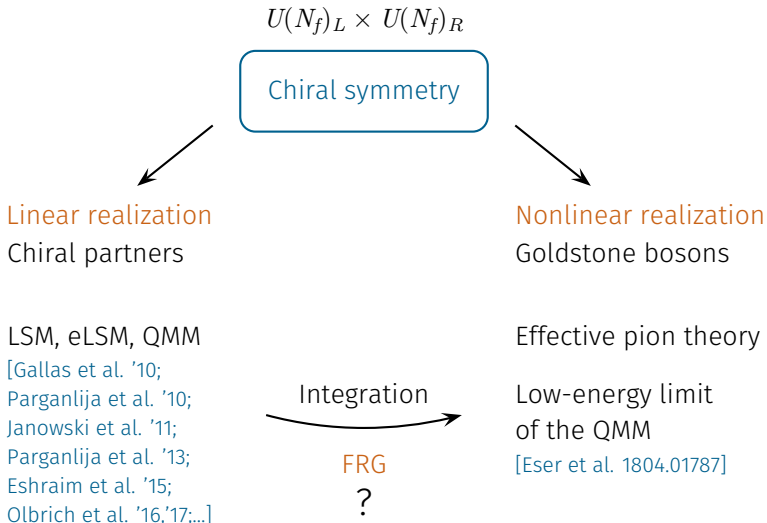
Low-energy limit of the $O(4)$ quark-meson model

Jürgen Eser, Florian Divotgey, Mario Mitter, and Dirk H. Rischke

Lunch Club Seminar

Giessen | April 18, 2018

Motivation



$O(4)$ quark-meson model (QMM)

- Two-flavor model, $N_f = 2$
- Euclidean action:

$$S = \int_x \left\{ \frac{1}{2} (\partial_\mu \sigma) \partial_\mu \sigma + \frac{1}{2} (\partial_\mu \vec{\pi}) \cdot \partial_\mu \vec{\pi} \right. \\ \left. + U(\rho) - h_{\text{ESB}} \sigma \right. \\ \left. + \bar{\psi} (\gamma_\mu \partial_\mu + y \Phi_5) \psi \right\},$$

$$\Phi_5 = \sigma t_0 + i \gamma_5 \vec{\pi} \cdot \vec{t},$$

$$\rho = \sigma^2 + \vec{\pi}^2$$

- **Explicit** and **spontaneous** symmetry breaking implemented:

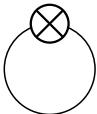
$$h_{\text{ESB}} \neq 0,$$

$$\sigma \rightarrow \phi + \sigma$$

Integration within the FRG

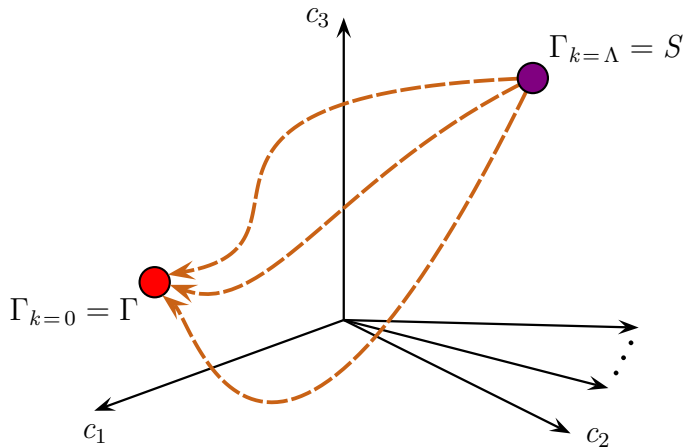
Functional renormalization group (FRG)

- Implementation of the **Wilsonian RG** idea
- Renormalization scale(k)-dependent **effective action** Γ_k
- FRG flow equation [**Wetterich '93**]:

$$\partial_k \Gamma_k = \frac{1}{2} \text{tr} \left[\partial_k R_k \left(\Gamma_k^{(2)} + R_k \right)^{-1} \right] = \frac{1}{2} \text{tr} \left[\partial_k R_k \left(\Gamma_k^{(2)} + R_k \right)^{-1} \right]$$
A Feynman diagram representing a tadpole loop. It consists of a circle with a small circle attached to its top edge. The small circle contains an 'X' symbol, representing a regulator insertion.

- Regulator function R_k provides correct integration limits

Flow in theory space



Effective action

- Introduce low-energy couplings:

$$\Gamma_k = \int_x \left\{ \frac{Z_k^\sigma}{2} (\partial_\mu \sigma) \partial_\mu \sigma + \frac{Z_k^\pi}{2} (\partial_\mu \vec{\pi}) \cdot \partial_\mu \vec{\pi} \right. \\ + U_k(\rho) - h_{\text{ESB}} \sigma \\ + C_{2,k} (\vec{\pi} \cdot \partial_\mu \vec{\pi})^2 + Z_{2,k} \vec{\pi}^2 (\partial_\mu \vec{\pi}) \cdot \partial_\mu \vec{\pi} \\ - C_{3,k} [(\partial_\mu \vec{\pi}) \cdot \partial_\mu \vec{\pi}]^2 - C_{4,k} [(\partial_\mu \vec{\pi}) \cdot \partial_\nu \vec{\pi}]^2 \\ - C_{5,k} \vec{\pi} \cdot (\partial_\mu \partial_\mu \vec{\pi}) (\partial_\nu \vec{\pi}) \cdot \partial_\nu \vec{\pi} \\ - C_{6,k} \vec{\pi}^2 (\partial_\mu \partial_\nu \vec{\pi}) \cdot \partial_\mu \partial_\nu \vec{\pi} \\ - C_{7,k} (\vec{\pi} \cdot \partial_\mu \partial_\mu \vec{\pi})^2 - C_{8,k} \vec{\pi}^2 (\partial_\mu \partial_\mu \vec{\pi})^2 \\ \left. + \bar{\psi} \left(Z_k^\psi \gamma_\mu \partial_\mu + y \Phi_5 \right) \psi \right\}$$

- $C_{1,k}(\vec{\pi}^2)^2$ is part of the effective potential U_k
- Goal: Compute the IR values of $C_{1,k}$, $C_{2,k}$, $Z_{2,k}$, and $C_{3,k}, \dots, C_{8,k}$

Low-energy limit

- Equation of motion (renormalized quantities):

$$\frac{\delta\Gamma}{\delta\tilde{\sigma}} = 0$$

- Effective pion action:

$$\begin{aligned} \Gamma_k = \int_x \left\{ \frac{1}{2} \left(\partial_\mu \tilde{\pi} \right) \cdot \partial_\mu \tilde{\pi} + \frac{1}{2} M_{\pi,k}^2 \tilde{\pi}^2 - \tilde{C}_{1,k}^{\text{total}} \left(\tilde{\pi}^2 \right)^2 \right. \\ + \tilde{C}_{2,k}^{\text{total}} \left(\tilde{\pi} \cdot \partial_\mu \tilde{\pi} \right)^2 + \tilde{Z}_{2,k}^{\text{total}} \tilde{\pi}^2 \left(\partial_\mu \tilde{\pi} \right) \cdot \partial_\mu \tilde{\pi} \\ - \tilde{C}_{3,k}^{\text{total}} \left[\left(\partial_\mu \tilde{\pi} \right) \cdot \partial_\mu \tilde{\pi} \right]^2 - \tilde{C}_{4,k}^{\text{total}} \left[\left(\partial_\mu \tilde{\pi} \right) \cdot \partial_\nu \tilde{\pi} \right]^2 \\ - \tilde{C}_{5,k}^{\text{total}} \tilde{\pi} \cdot \left(\partial_\mu \partial_\mu \tilde{\pi} \right) \left(\partial_\nu \tilde{\pi} \right) \cdot \partial_\nu \tilde{\pi} \\ - \tilde{C}_{6,k}^{\text{total}} \tilde{\pi}^2 \left(\partial_\mu \partial_\nu \tilde{\pi} \right) \cdot \partial_\mu \partial_\nu \tilde{\pi} \\ \left. - \tilde{C}_{7,k}^{\text{total}} \left(\tilde{\pi} \cdot \partial_\mu \partial_\mu \tilde{\pi} \right)^2 - \tilde{C}_{8,k}^{\text{total}} \tilde{\pi}^2 \left(\partial_\mu \partial_\mu \tilde{\pi} \right)^2 \right\} \end{aligned}$$

Flow equations

$$\partial_k U_k = \mathcal{V}^{-1} \left(\frac{1}{2} \text{diagram}_\sigma + \frac{1}{2} \text{diagram}_\pi - \text{diagram}_\psi \right),$$

$$\partial_k Z_k^\pi = \mathcal{V}^{-1} \frac{d}{dp^2} \Big|_{p^2=0} \left(\frac{1}{2} \text{diagram}_{\sigma,3} - \frac{1}{2} \text{diagram}_{\pi,4} + \dots \right),$$

$$\partial_k C_{2,k} = \mathcal{V}^{-1} \frac{d}{dp^2} \Big|_{p^2=0} \left(-\frac{1}{2} \text{diagram}_{\sigma,3} + \dots \right),$$

⋮

Symmetry breaking and renormalized masses

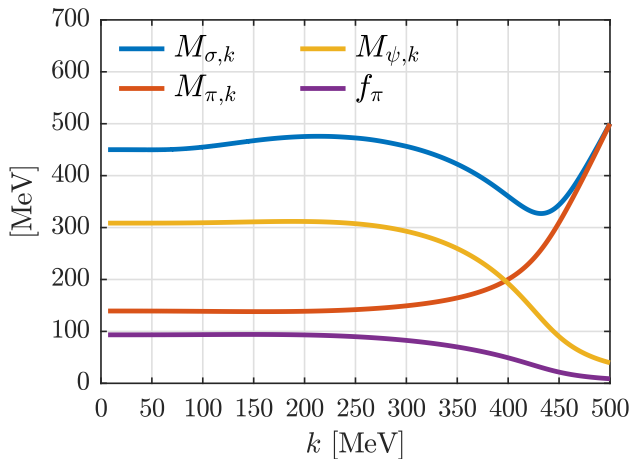


Figure 1: Scale evolution of the renormalized meson and quark masses and the pion decay constant; $k_{\text{IR}} = 7$ MeV; [1804.01787].

Wave-function renormalization

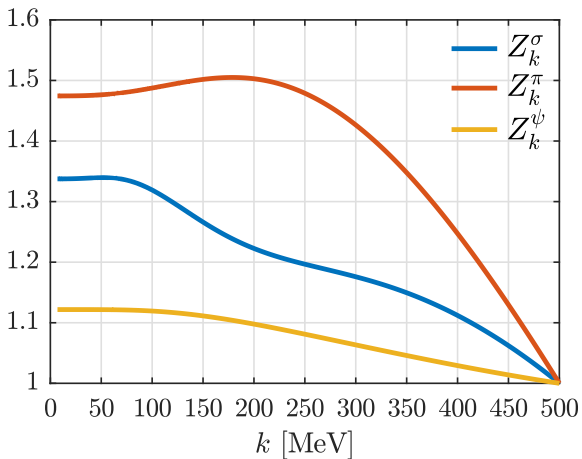


Figure 2: Scale evolution of the wave-function renormalization factors Z_k^σ , Z_k^π , and Z_k^ψ ; $k_{\text{IR}} = 7$ MeV; [1804.01787].

Pion self-interactions $\mathcal{O}(\partial^2)$

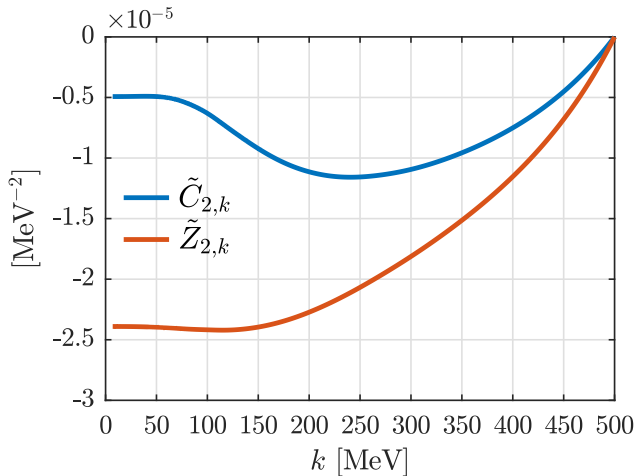


Figure 3: Scale evolution of the momentum-dependent pion self-interactions of the order $\mathcal{O}(\partial^2)$; $k_{\text{IR}} = 7$ MeV; [1804.01787].

Pion self-interactions $\mathcal{O}(\partial^4)$

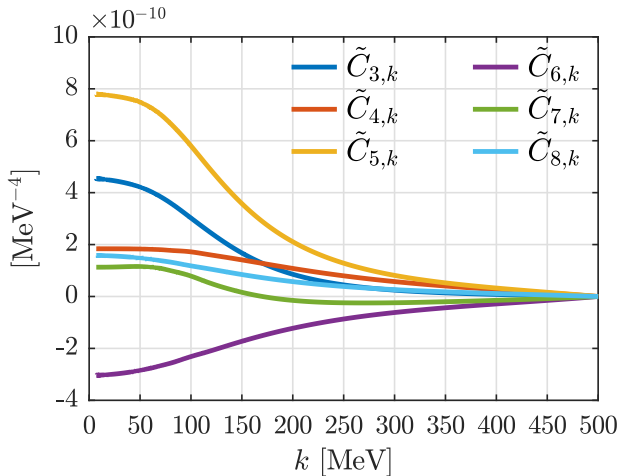


Figure 4: Scale evolution of the momentum-dependent pion self-interactions of the order $\mathcal{O}(\partial^4)$; $k_{\text{IR}} = 7 \text{ MeV}$; [1804.01787].

Numerical results

Table 1: Low-energy couplings ($f_\pi = 93$ MeV); [1804.01787].

| Coupling | Tree level | FRG | | |
|-------------------------------|------------|--------|---------|---------|
| | | tree | trunc | total |
| C_1 | -0.2514 | 2.1063 | -2.3550 | -0.2487 |
| $C_2 [1/f_\pi^2]$ | 0.4054 | 0.3598 | -0.0426 | 0.3172 |
| $Z_2 [1/f_\pi^2]$ | - | - | -0.2068 | -0.2068 |
| $C_3 [1/f_\pi^4] \times 10^2$ | 1.7311 | 1.5364 | 3.3946 | 4.9310 |
| $C_4 [1/f_\pi^4] \times 10^2$ | - | - | 1.3752 | 1.3752 |
| $C_5 [1/f_\pi^4] \times 10^2$ | 3.4621 | 3.0728 | 5.8294 | 8.9023 |
| $C_6 [1/f_\pi^4] \times 10^2$ | - | - | -2.2697 | -2.2697 |
| $C_7 [1/f_\pi^4] \times 10^2$ | 1.7311 | 1.5364 | 0.8439 | 2.3804 |
| $C_8 [1/f_\pi^4] \times 10^2$ | - | - | 1.1828 | 1.1828 |

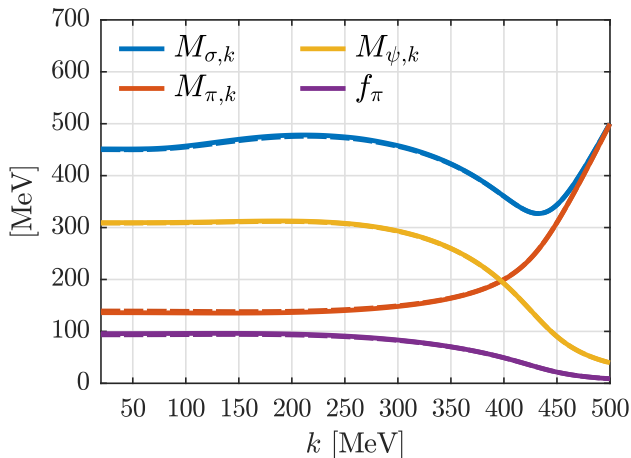


Figure 5: Scale evolution of the renormalized meson and quark masses within the LPA' truncation. The dashed lines show the related results from Fig. 1; $k_{\text{IR}} = 20$ MeV; [1804.01787].

LPA' wave-function renormalization

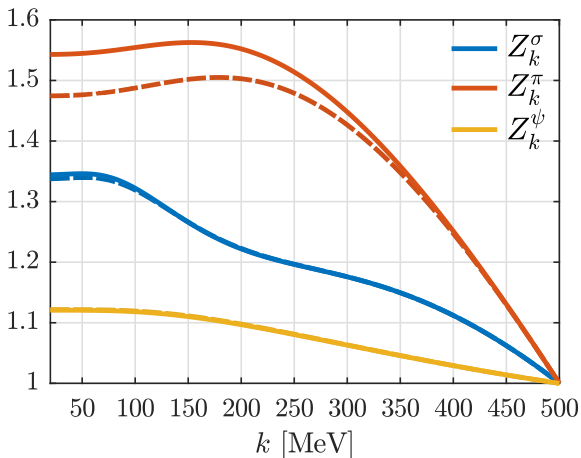


Figure 6: Scale evolution of the wave-function renormalization factors Z_k^σ , Z_k^π , and Z_k^ψ within the LPA' truncation. The dashed lines show the related results from Fig. 2; $k_{\text{IR}} = 20$ MeV; [1804.01787].

Outlook

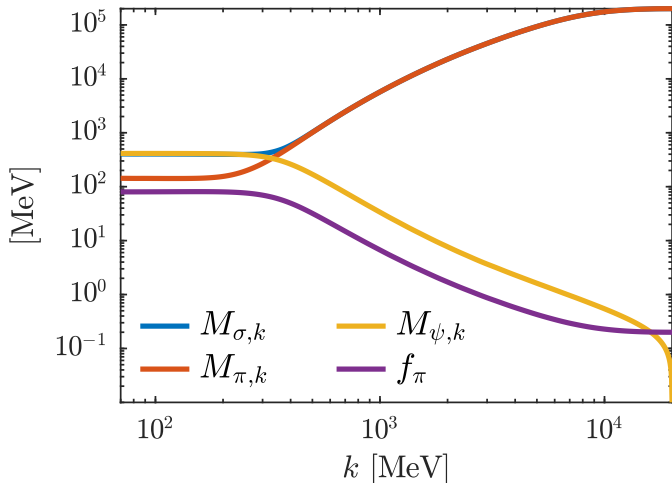


Figure 7: Scale evolution of the renormalized meson and quark masses and the pion decay constant; $k_{\text{IR}} = 70$ MeV.

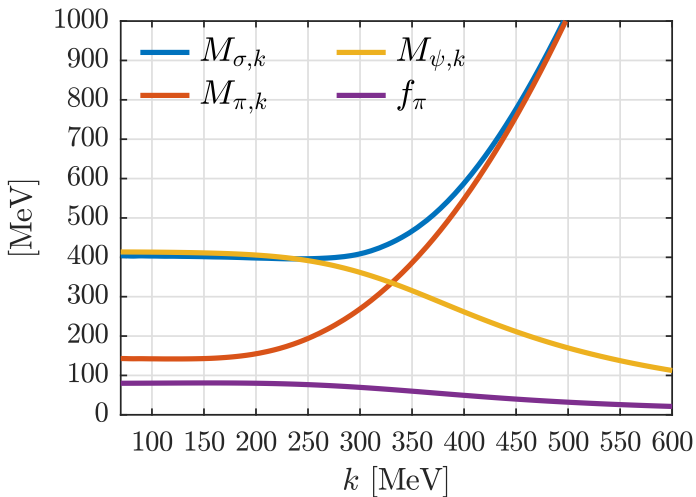


Figure 8: Scale evolution of the renormalized meson and quark masses and the pion decay constant; $k_{\text{IR}} = 70$ MeV.

QCD wave-function renormalization

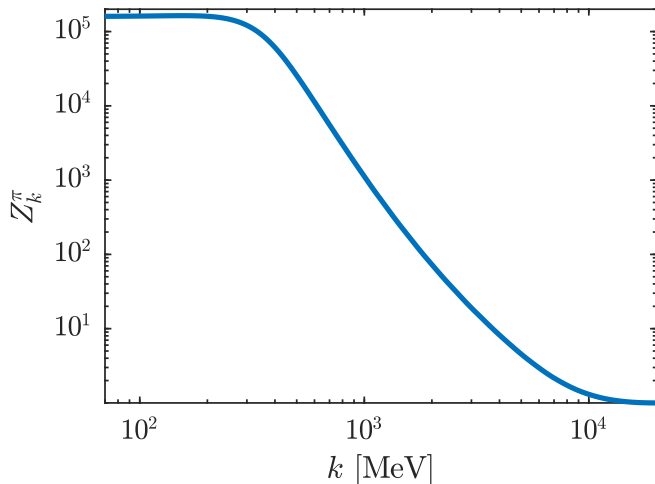


Figure 9: Scale evolution of the pion wave-function renormalization; $k_{\text{IR}} = 70$ MeV.

QCD wave-function renormalization

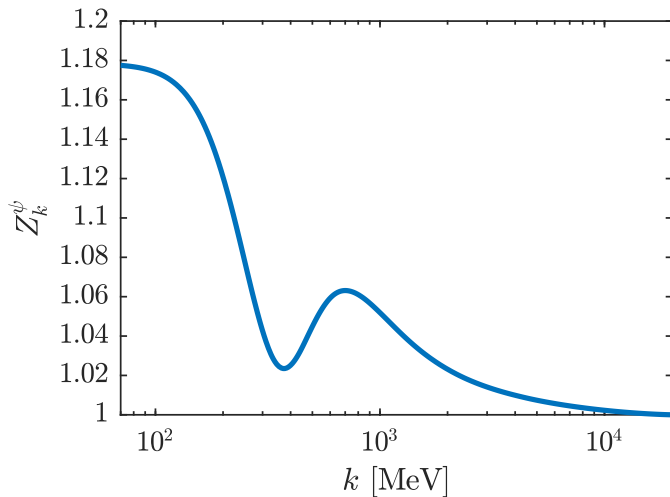


Figure 10: Scale evolution of the quark wave-function renormalization; $k_{\text{IR}} = 70$ MeV.

Pion self-interactions from QCD

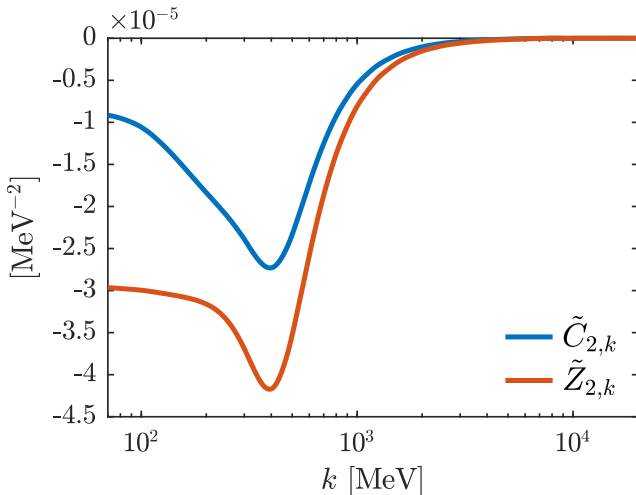


Figure 11: Scale evolution of the momentum-dependent pion self-interactions of the order $\mathcal{O}(\partial^2)$; $k_{\text{IR}} = 70$ MeV.

Pion self-interactions from QCD

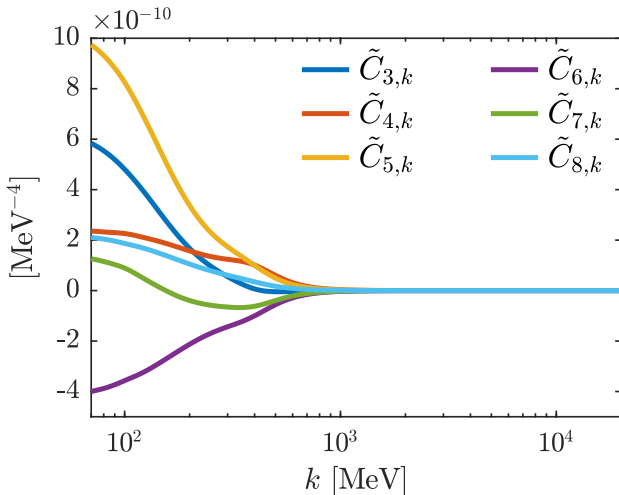


Figure 12: Scale evolution of the momentum-dependent pion self-interactions of the order $\mathcal{O}(\partial^4)$; $k_{\text{IR}} = 70$ MeV.

Table 2: Low-energy couplings from QCD input.

| Coupling | Tree level | FRG | |
|-------------------------------|------------|---------|---------|
| | | $O(4)$ | QCD |
| C_1 | -0.2514 | -0.2487 | -0.3479 |
| $C_2 [1/f_\pi^2]$ | 0.4054 | 0.3172 | 0.4372 |
| $Z_2 [1/f_\pi^2]$ | - | -0.2068 | -0.2565 |
| $C_3 [1/f_\pi^4] \times 10^2$ | 1.7311 | 4.9310 | 7.1016 |
| $C_4 [1/f_\pi^4] \times 10^2$ | - | 1.3752 | 1.7625 |
| $C_5 [1/f_\pi^4] \times 10^2$ | 3.4621 | 8.9023 | 12.7534 |
| $C_6 [1/f_\pi^4] \times 10^2$ | - | -2.2697 | -2.9918 |
| $C_7 [1/f_\pi^4] \times 10^2$ | 1.7311 | 2.3804 | 3.6749 |
| $C_8 [1/f_\pi^4] \times 10^2$ | - | 1.1828 | 1.5770 |

Chiral perturbation theory (ChPT)

Compare low-energy couplings of the **extended LSM (eLSM)**:

- Chiral expansion of the QCD generating functional (ChPT [Gasser, Leutwyler '84,'85; Leutwyler '94;...]):

$$\begin{aligned}\mathcal{L}_{\text{ChPT}} = & \frac{1}{2} (\partial_\mu \vec{\pi})^2 - \frac{1}{2} m_\pi^2 \vec{\pi}^2 + C_{1,\text{ChPT}} (\vec{\pi}^2)^2 + C_{2,\text{ChPT}} (\vec{\pi} \cdot \partial_\mu \vec{\pi})^2 \\ & + C_{3,\text{ChPT}} (\partial_\mu \vec{\pi})^2 (\partial_\nu \vec{\pi})^2 + C_{4,\text{ChPT}} (\partial_\mu \vec{\pi} \cdot \partial_\nu \vec{\pi})^2 \\ & + \mathcal{O}(\pi^6, \partial^6)\end{aligned}$$

- Low-energy limit of the eLSM at tree level [Divotgey et al. '18]:

$$\begin{aligned}\mathcal{L}_{\text{eLSM}} = & \frac{1}{2} (\partial_\mu \vec{\pi})^2 - \frac{1}{2} m_\pi^2 \vec{\pi}^2 + C_{1,\text{eLSM}} (\vec{\pi}^2)^2 + C_{2,\text{eLSM}} (\vec{\pi} \cdot \partial_\mu \vec{\pi})^2 \\ & + C_{3,\text{eLSM}} (\partial_\mu \vec{\pi})^2 (\partial_\nu \vec{\pi})^2 + C_{4,\text{eLSM}} (\partial_\mu \vec{\pi} \cdot \partial_\nu \vec{\pi})^2 \\ & + \mathcal{O}(\pi^6, \partial^6)\end{aligned}$$

Table 3: Comparison of the low-energy couplings at tree level, cf. [Bijnens, Ecker '14; Divotgey et al. '18].

| Coupling | ChPT | eLSM |
|------------------------------------|-------------------|---------------------------------|
| C_1 | -0.29 ± 0.34 | -0.268 ± 0.021 |
| $C_2 \times 10^5 \text{ MeV}^2$ | 5.882 ± 0.013 | 5.399 ± 0.081 |
| $C_3 \times 10^{11} \text{ MeV}^4$ | -5.57 ± 0.88 | $-9.30 \pm 0.59 + \text{corr.}$ |
| $C_4 \times 10^{11} \text{ MeV}^4$ | 2.58 ± 0.29 | $9.45 \pm 0.59 + \text{corr.}$ |

- How do these values change if we include **loop corrections**?
- Can we produce similar values within the **FRG formalism**?

Summary

Summary

Summary:

- Low-energy limit of the $O(4)$ quark-meson model within the FRG confronted with a tree-level estimate
- Discrepancy between these approaches observed
- Low-energy couplings of the eLSM at tree level in good agreement with ChPT, cf. [Bijnens, Ecker '14; Divotgey et al. '18]

Upcoming:

- Extend analysis to the full $O(4)$ -symmetric scenario
- Include vector mesons and scale-dependent Yukawa coupling
- Compute low-energy limit from first-principles QCD
- Confront the FRG calculation with ChPT